Deep Space GNSS in Moon Transfer Orbit: the LuGRE Receiver

Designing Deep Space GNSS in Moon Transfer Orbit: the LuGRE Receiver

Simone Tedesco, Fabio Bernardi, Salvatore Guzzi, Matilde Boschiero, Matteo Pulliero, Davide Marcantonio, Mattia Ghedin, Efer Miotti, Samuele Fantinato, Oscar Pozzobon
Qascom Srl
Bassano Del Grappa, Italy
simone.tedesco@qascom.it, fabio.bernardi@qascom.it, salvatore.guzzi@qascom.it, matilde.boschiero@qascom.it, matteo.pulliero@qascom.it, davide.marcantonio@qascom.it, mattia.ghedin@qascom.it, efer.miotti@qascom.it, samuele.fantinato@qascom.it, oscar.pozzobon@qascom.it

Claudia Facchinetti, Mario Musmeci, Giuseppe D'Amore, Giancarlo Varacalli; Alex Minetto, Fabio Dovis
Agenzia Spaziale Italiana; Politecnico di Torino
Roma; Torino, Italy
claudia.facchinetti@asi.it, mario.musmeci@asi.it, giuseppe.damore@asi.it, giancarlo.varacalli@asi.it; alex.minetto@polito.it, fabio.dovis@polito.it

Joel J. K. Parker, Stephen A.McKim, Lauren Konitzer, Benjamin Ashman, Siddartha Sanathanamurthy
NASA Goddard Space Flight Center
Greenbelt, Maryland, USA
joel.j.k.parker@nasa.gov, stephen.a.mckim@nasa.gov, lauren.konitzer@nasa.gov, benjamin.w.ashman@nasa.gov, siddartha.sanathanamurthy@nasa.gov

James J. Miller, Lisa Valencia; Frank Bauer
NASA Headquarters; FBauer Aerospace Consulting Services
Washington, DC; Maryland, USA
jj.miller@nasa.gov, lisa.m.valencia@nasa.gov; frank.h.bauer@nasa.gov

***Abstract*—The Lunar GNSS Receiver Experiment (LuGRE) is a payload developed as part of the NASA Commercial Lunar Payload Services (CLPS) program as a partnership between the Italian Space Agency (ASI) and the National Aeronautics and Space Administration (NASA). The main objective of the project is to achieve GNSS-based Positioning, Navigation, and Timing (PNT) during the Moon Transfer Orbit (MTO) and, finally, on the Moon's Surface (MS). The project focused on the development of a GNSS Software Defined Radio (SDR) receiver, which is a Moon-customized version of the Qascom QN400-SPACE. The receiver logic has been refined with specific features that permit it to operate properly in deep-space environments. High-sensitivity acquisition and tracking techniques have been embedded to acquire and track GNSS signals at higher altitudes. Specialized Navigation plugins have been added for MTO and static MS positioning. This paper aims to present and analyze the most significant results obtained during the LuGRE receiver test campaign. The test scenarios are presented to provide a fruitful comparison between the receiver's real and expected performance.**

Keywords—LuGRE, GNSS, receiver, moon, PNT

I. Introduction

The application of Global Navigation Satellite Systems (GNSS), currently in-orbit in the Space Service Volume (SSV), for future lunar missions has recently gained a significant momentum.

The Lunar GNSS Receiver Experiment (LuGRE) is a payload developed by Qascom S.r.l within the CLPS Task 19D, in collaboration with NASA and ASI. LuGRE will fly on board of the US Firefly Blue Ghost Mission 1 Lander (BGM1), landing on the Moon's Mare Crisium in 2024. LuGRE's goal is to extend GNSS-based navigation and timing to the Moon. During its operations, LuGRE will use GPS and Galileo measurements to achieve the first GNSS fix in lunar and cislunar environments. LuGRE will demonstrate the feasibility of on-board real-time positioning and navigation solutions using GNSS signals at lunar distance.

The LuGRE project oversaw the development of a dual-constellation and dual-frequency GNSS Software Defined Radio (SDR) receiver based on the Qascom QN400-Space specifically adapted for MTO and MS scenarios. The payload contained also a High-Gain Antenna (HGA) and a Front-End Assembly (FEA), containing a multi-stage Low Noise Amplifier (LNA) with dual-band filtering at L1 and L5.

This paper describes the challenges faced during the project to optimize the LuGRE GNSS receiver to acquire and track signals in deep space. Chapter II depicts the state of the art, addressing the current perspective on the use of GNSS for future lunar applications. As part of the LuGRE payload validation, several tests have been performed to verify the GNSS SDR receiver functionalities and performance. The MTO and MS scenarios used to theoretically characterize the mission are presented in Chapter III. The high-sensitivity logic employed by the receiver is discussed in Chapter IV, while the results of the validation tests are analyzed in Chapter V.

II. State of the Art

The use of GNSS signals for spacecraft navigation is a common practice in Low Earth Orbit (LEO) [1] and it is raising increasing interest for higher orbits scenarios [2].

The LuGRE mission will pave the way for the development of GNSS-based navigation for transit orbits towards the Moon and on its surface. Hence, NASA and the European Space Agency (ESA) have outlined plans for a lunar navigation infrastructure that incorporates GNSS technology for cislunar and lunar navigation [3] [4]. Despite the GNSS reliability proven in these recent years [5], there are several challenges to be acknowledged when considering the

exploitation of this technology at these higher altitudes in space. The corresponding degradation in signal performance, due to the distance and the geometry of the scenario, could severely limit the resulting GNSS usability.

To overcome these challenges, a phased approach is required. The first step focuses on evaluating the integration of GNSS technology into the lunar navigation through the use of reliable flight demonstrations [6] [7] [8]. As such, LuGRE is perfectly placed within this scope. Subsequently, the heritage acquired during the first stage will lead to the development of operational lunar GNSS receivers, deployed in-orbit or on the Moon' surface [6]. Finally, ESA's initiative called Moonlight [9] will aim to establish a fully operational lunar GNSS navigation infrastructure capable of real-time navigation solutions from near-Earth to the lunar surface.

Nevertheless, developing a fully integrated navigation system of such magnitude is an incredibly ambitious project that requires a combined effort and a multidisciplinary interest from different stakeholders, including academia, industry, and government agencies.

III. Mission Scenarios

The LuGRE payload has been designed as power-efficient, robust, low-mass system able to withstand the severe conditions experienced throughout the BGM1 lander journey to the Moon. It consists of:

- A High-Gain Antenna (HGA), optimized for GNSS L1/E1 and L5/E5a bands. The design was tailored for acquisition and tracking degraded signals in deep space. Moreover, it included an embedded filtering stage to limit the interference out of band.
- A Front-End Assembly (FEA), incorporating in series a pre-selection band pass filter (BPF), followed by a Low-Noise Amplifier (LNA) and an equalizer (EQ), designed to isolate the receiving signals from noise and interferences.
- The QN400-SPACE receiver, Qascom's multi-constellation (GPS/Galileo) and multi-frequency (L1/L5) GNSS receiver, optimized for high-sensitivity acquisition at higher altitudes.
- Coaxial harnesses and cabling connecting all payload elements to each other and to the BGM1 lander.

The theoretical LuGRE payload performance in space has been simulated in a synthetic environment, emulating the mission scenarios of interest. Several points in the Moon Transfer Orbit (MTO) trajectories can be selected, as well as in Low Lunar Orbit (LLO) and in Moon Surface (MS). The results presented in this paper refers to a point of choice at a distance from Earth equals to 30 Radius Earth (RE).

The work of Delépaut et al. [10] allowed to draw the values of the EIRP, presented in Figure 1 and Figure 2. From this, the transmitting antenna pattern was derived and applied to the gain measurements, provided by Marquis et al. [11] for the GPS IIR and IIR-M blocks. The antenna radiation of the GPS IIF batches from Boeing were extracted from [12]. Due to the lack of available data at the time of the experiment, the same pattern was used as an approximation for the Block III-A. Regarding Galileo, the patterns were analytically computed considering the GPS IIF batch and adjusted with a corrective parameter relative to the difference in altitude of the two constellations.

The Link Budget was assessed by estimating the Carrier-to-Noise Ratio (C/N_0), simulating the impact of the communication losses, and the relative RF chain, on the received signals. The GNSS input signals were generated using a Radio Frequency Constellation Simulator (RFCS), and the considered signal degradation accounted for the Free Space Path Loss (FSPL), the receiving HGA gain, the LNA noise figure and the RF chain losses.

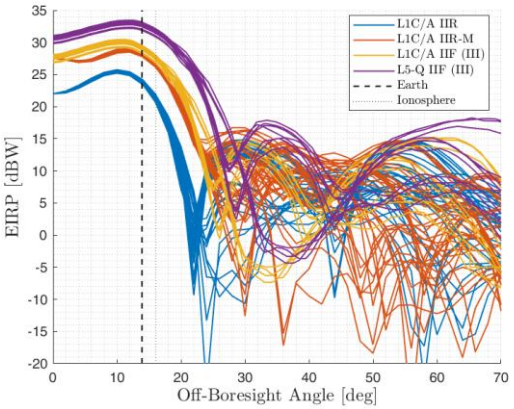

Figure 1: EIRP Antenna Patterns for GPS [10]

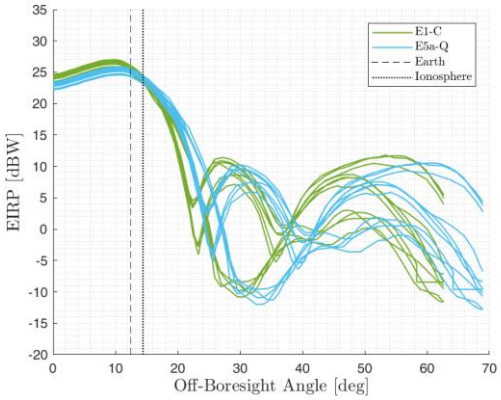

Figure 2: EIRP Antenna Patterns for Galileo [10]

The C/N_0 was simulated for both the main and side lobes in order to properly compare the final QN400-SPACE GNSS receiver performance in space.

IV. High-Sensitivity GNSS Receiver

The following chapter will dive into details of the high-sensitivity features developed for the LuGRE GNSS receiver and tailored to acquire the weak signals at lunar altitude in space.

A. High-Sensitivity Acquisition

The first stage of the processing block in the architecture of a traditional GNSS receiver is the signal acquisition. It aims at obtaining a rough estimates of Doppler frequencies and code phases of the received GNSS signals, later employed in the tracking stage. The QN400-SPACE receiver employs the coherent and the non-coherent acquisition schemes [3]. These two schemes can be combined to improve the acquisition performance, especially when the process is performed in harsh environments. Indeed, one of the main challenges for

acquisition during navigation towards the Moon is represented by the weak GNSS signal power available at the on-board GNSS receiver. Therefore, high-sensitivity acquisition strategies are required to deal with reduced received power. The proposed strategy is based on the two-stage scheme highlighted in the flow-chart of Figure 3 and detailed below.

The first step is to acquire the satellite with the estimated highest received power. The search is performed over a large frequency range to track the signal Doppler frequency even with a high residual Doppler error. This is achieved by keeping the coherent integration time as low as possible while increasing the number of non-coherent integrations.

The second acquisition stage is used to acquire signals at lower power. Here the Doppler space can be reduced by estimating the unknown clock drift from the first satellite tracked. This stage is performed by keeping the number of non-coherent integrations low and increasing the coherent integration time.

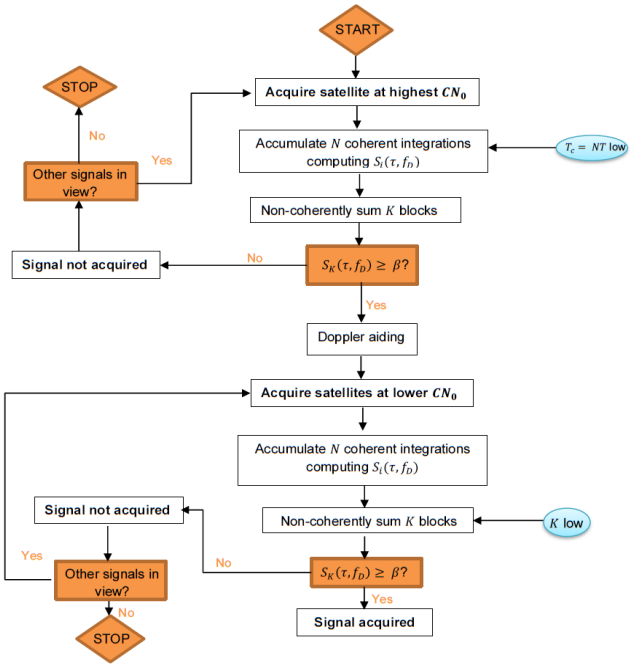

Figure 3: High-sensitivity Acquisition Logic

B. *High-Sensitivity Tracking*

The coarse estimates of the signal frequency and code phase provided by the acquisition module are refined during the tracking phase. Indeed, the tracking module refined the estimates, follows signals dynamics, demodulates the navigation data bits and, eventually, it generates the GNSS raw measurements. The baseband (BB) complex signal, after down-conversion, enters the tracking stage of the receiver. Then, it is multiplied by the local replica of the carrier, in order to remove the signal Doppler shift and local oscillator frequency error. The signal is then multiplied with the shifted local replicas of the PRN code and integrated (Integrate & Dump, I&D), in order to generate the early (E), prompt (P), and late (L) correlation values. These values are fed to the Code and Carrier discriminators. The aim of discriminators is to estimate the code phase, frequency, and carrier phase tracking errors. The tracking errors are then filtered by the code and carrier loop filters, whose output is used to control the generation of the local carrier and code replicas. QN400-Space integrates a second-order carrier-aided delay lock loop (DLL) for code phase tracking, a second-order frequency lock loop (FLL) and a third-order phase lock loop (PLL) for carrier frequency and phase tracking, respectively [13]. The overall tracking architecture is shown in Figure 4. The Carrier Loop Filter consists in a Frequency-aided PLL (FAP).

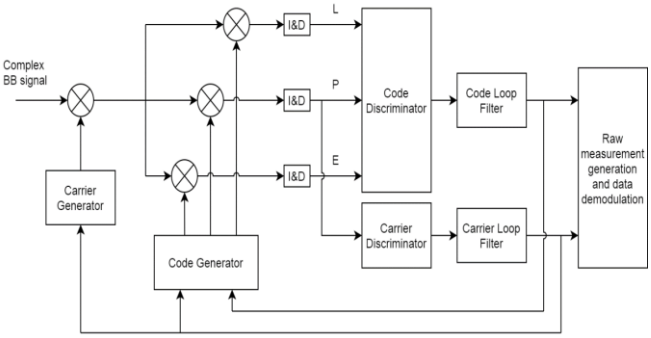

Figure 4: Tracking Architecture

In order to improve the receiver sensitivity, a semi-analytical analysis was carried out by systematically testing and optimizing the tracking loop performance. The analysis consists of generating a software-based GNSS signal that has undergone unique processing within the receiver's tracking stage. The signal generation process considers the presence of thermal noise, while the influence of additional factors, such as the Allan deviation of the clock, has been disregarded for the purpose of this analysis. This controlled environment allows the receiver's tracking performance to be carefully evaluated and improved in a way that is easy to evaluate.

The signal generator can simulate signal parameters based on input C/N0 and Doppler profiles.

Hence, the input signal is directly fed into the tracking stage of the receiver, bypassing the acquisition stage but considering a possible error in the acquisition estimates. A starting Doppler value is manually set to correspond to the acquired Doppler, effectively initializing the tracking process. The difference between the starting Doppler and the actual Doppler is defined as the Doppler error during acquisition. The maximum error is equal to half of the Doppler resolution in the acquisition stage, which, in our case, is fixed at 9 Hz.

Therefore, the tracking loop outputs are analyzed to determine if the receiver has established and maintained a reliable connection with the satellite signal, indicating successful tracking lock. This latter is crucial for GNSS receivers as it enables accurate determination of position, velocity, and timing information. Once tracking lock is achieved, the receiver can extract and demodulate the navigation data embedded in the satellite signals.

The declaration of tracking lock is based on the assessment of phase jitter or tracking jitter. The phase jitter is estimated by computing the standard deviation of the carrier phase tracking error. Lock is declared when the phase jitter falls below a predetermined threshold, which, in our case, is set to 30° [13].

Subsequently, a Monte Carlo simulation has been performed to optimize the tracking loops parameters, namely the filter bandwidths and the weights of the Frequency-Locked Loop (FLL) and the Phase-Locked Loop (PLL). In detail, a signal with C/N0 equal to 23 dB-Hz was generated using the semi-analytical signal generator and processed by

the receiver over 1000 iterations. The tracking lock success rate was then calculated as the ratio of the number of successful locks to the total number of simulations. This process was repeated, varying the above parameters, and the combination with the highest success rate was selected. The results suggest that reducing the filter bandwidths and giving less weight to the FLL in the FAP contributes to more robust tracking performance in the presence of noise.

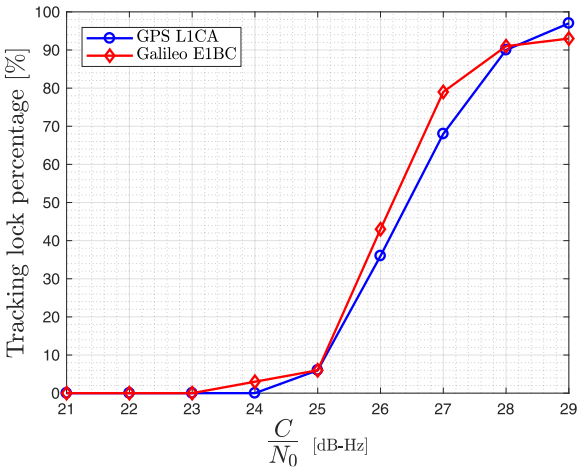

Figure 5: Tracking Lock Percentage over C/N0 before Optimization

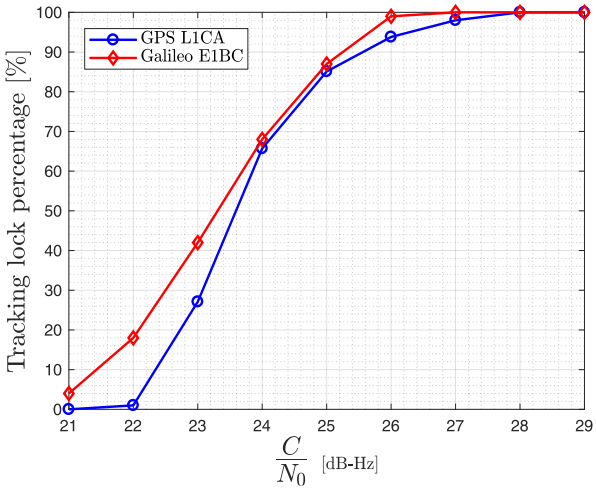

Figure 6: Tracking Lock Percentage over C/N0 after Optimization

Finally, Figure 5 and Figure 6 illustrate a comparison between the receiver performance before (top) and after (below) the optimization process, as a function of the tracking lock success rate over the C/N0. As presented in Figure 6, optimizing the tracking loops parameters led to a considerable increase in the tracking lock percentage. For instance, at a C/N0 ratio of 25 dB-Hz, the tracking lock percentage increased from around 8% to 85%. Similarly, considering a lower C/N0 of 23 dB-Hz, the tracking lock percentage improved of approximately 30%. In conclusion, these results demonstrated a significant improvement and increased robustness of the receiver performance due to the optimization process.

V. Test Results

The following chapter describes the receiver performance related to a MTO scenario, simulating the receiver position at a distance from Earth equal to 30 Radius Earth (RE). The RF chain considered a first harness from the Spirent GSS7000 RFCS signal generator to the LNA of 1.27 m, and a second harness from the LNA to the GNSS receiver of 0.23 m.

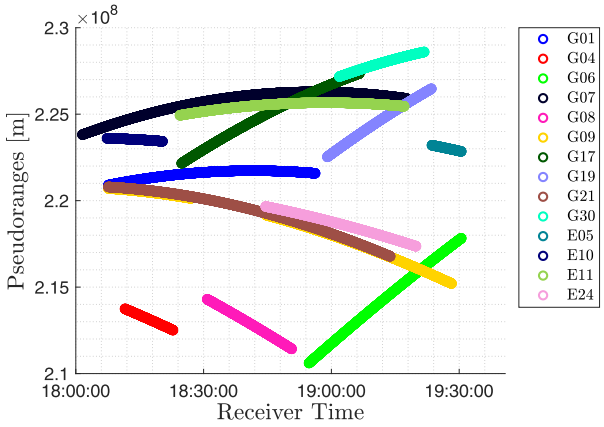

Figure 7: Pseudoranges in L1 Frequency

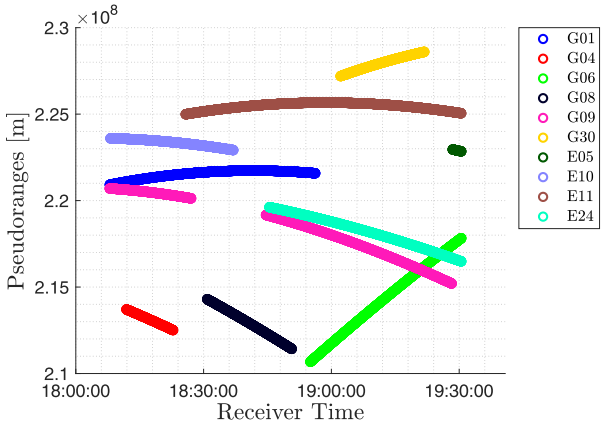

Figure 8: Pseudoranges in L5 Frequency

The real-time data generated by the receiver are then processed to obtain the following Key Performance Indicators (KPIs):

- Raw measurements as the pseudoranges, the carrier phases and doppler computed by the receiver.
- The number of L1/E1 and L5/E5 measurements used to compute a PVT solution.
- The position and velocity error profiles computed comparing the data generated by the receiver and the trajectory simulated by the RFCS.
- The Dilution of Precision (DOP).
- The PVT availability, computed as the amount of time in which the receiver generates a PVT solution over the scenario duration.

Figure 7 and Figure 8 show the pseudoranges computed by the receiver for both L1 and L5 for all the tracked satellites.

Figure 9 highlights the ability of the QN400-SPACE receiver to gather a number of measurements sufficient to compute the PVT for the whole duration of the 30 RE scenario. The PVT is computed using dual-frequency and dual-constellation measurements.

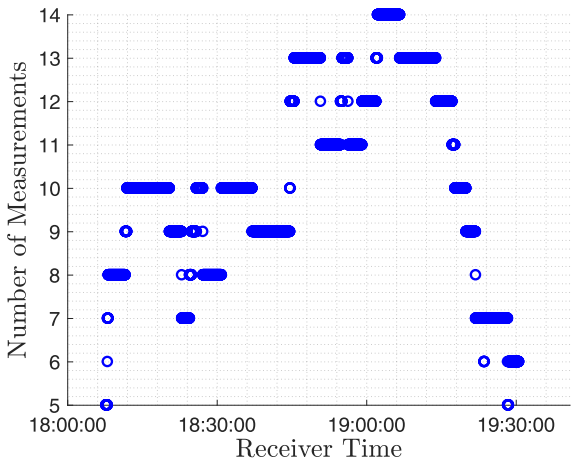

Figure 9: Number of Measurements used to compute PVT

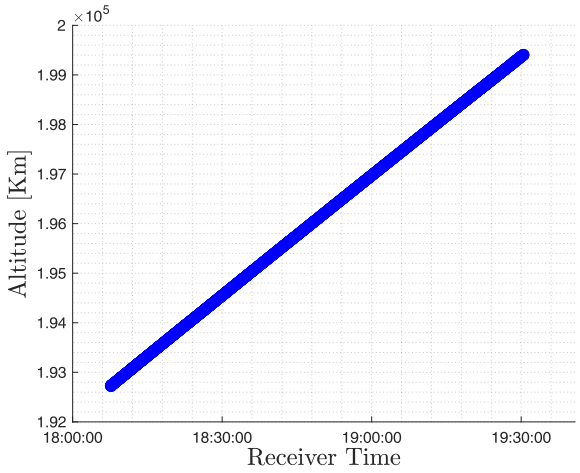

Figure 11: Altitude in Kilometers

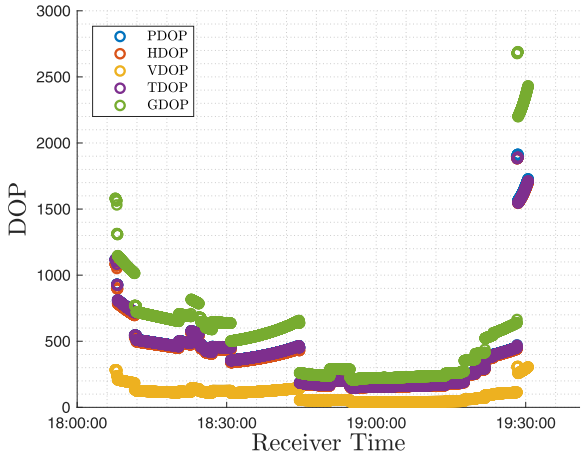

Figure 10: Dilution of Precision (DOP)

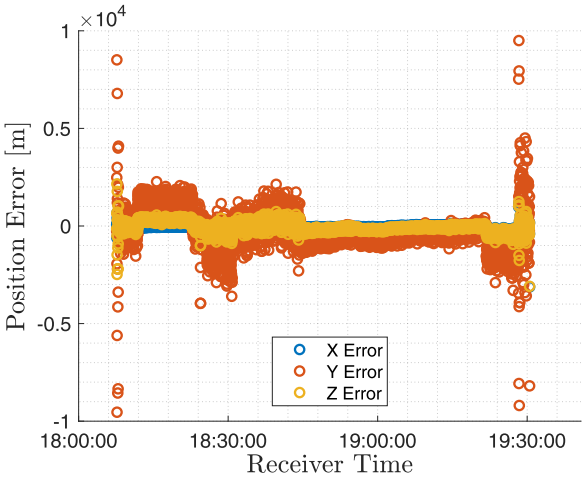

Figure 12: Position Error in Meters

Figure 10 shows the Dilution of Precision (DOP) computed by the receiver. The different types of DOP are represented using different color. Considerable importance is given by the Geometrical Dilution of Precision, or GDOP. Indeed, the goodness of the satellite's geometry, represented by the GDOP value has a strong impact on the GNSS positioning accuracy. As reported in [13], the GNSS positioning accuracy is directly proportional to the GDOP value. In lunar environments, the expected GDOP values are high due to the large distance from the Earth. These high values are confirmed by Figure 10.

Moreover, Figure 11 shows the altitude in kilometers computed by the receiver PVT algorithm. The altitude is coherent with the expectation at 30 RE from the Earth. In addition, Figure 12 plots the positioning error. This computation is performed in a fully simulated scenario where ground-truth (motion and satellite) data are available. When available, the navigation solution is computed by the receiver every second in ECEF reference system. It is important to note that the Position Error has a behavior comparable with the one of the DOP reported in Figure 10. Moreover, by comparing the two figures, it is possible to note that the position error decreases linearly with the GDOP. Finally, Figure 13 shows the velocity percent error.

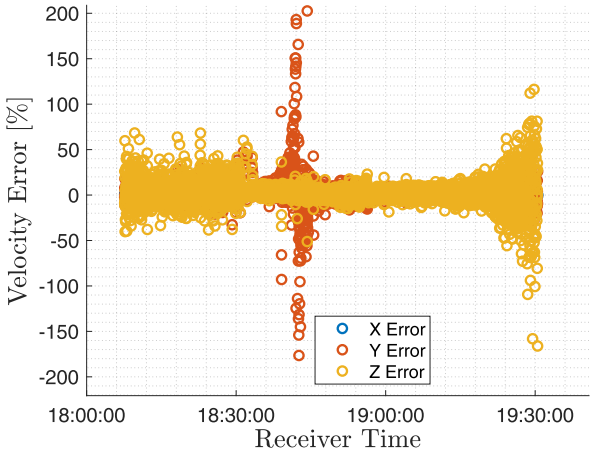

Figure 13: Velocity Percentage Error

The last analysis performed is a comparison between the satellites theoretically in view and the satellites acquired and tracked by the receiver. The combination between the scenario dynamic and the receiver's non-deterministic acquisition logic results in the performance presented in Figure 14 and Figure 15, respectively for GPS L1CA and GAL E1BC satellites.

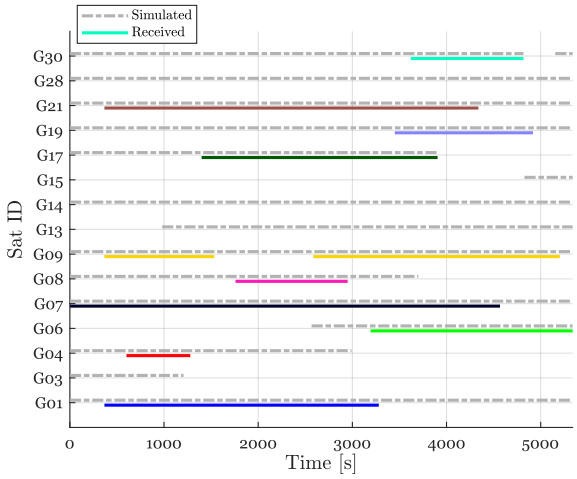

Figure 14: GPS L1CA Satellites Tracked during the Scenario

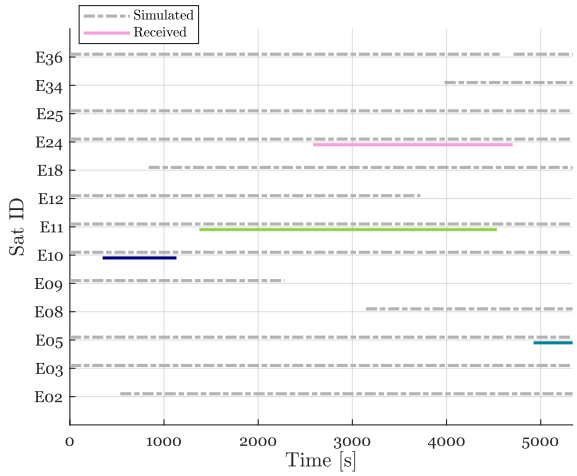

Figure 15: GAL E1BC satellites tracked during the scenario.

VI. Conclusion

The tests performed at 30 RE showed very promising results. The analysis performed on this scenario demonstrates that there is a good availability of satellites and, consequently, of measurements useful for performing a GNSS fix. The next step in the LuGRE tests will focus on assessing the receiver performance in scenarios at higher altitudes in lunar transfer orbit, as well as on the lunar surface. This will allow to characterize the receiver capability with a degraded geometry and lower satellite availability.

Acknowledgement

Qascom would like to acknowledge the teams in Firefly Aerospace, CLPS, NASA, ASI, and Politecnico of Torino for the exceptional technical and scientific support received for the LuGRE project.

References

[1] Bauer, F.H., Hartman, K. and Lightsey, E.G., 1998, March. Spaceborne GPS current status and future visions. In 1998 IEEE Aerospace Conference Proceedings (Cat. No. 98TH8339) (Vol. 3, pp. 195-208). IEEE

[2] Ashman, B., Bauer, F.H., Parker, J. and Donaldson, J., 2018. GPS operations in high earth orbit: Recent experiences and future opportunities. In 2018 SpaceOps Conference (p. 2568)

[3] Schönfeldt, Miriam & Swinden, Richard & Delépaut, Anaïs & Ventura-Traveset, Javier. (2020). Across the Lunar Landscape: Towards a Dedicated Lunar PNT System

[4] Israel D., "A LunaNet Implementation Approach", Proceedings of the 16th International Conference on Space Operations, SpaceOps 2021, May 2021

[5] The European Space Agency (ESA), ESA Navipedia, GNSS Market Report, Available at https://gssc.esa.int/navipedia/index.php/GNSS_Market_Report, Accessed on 05/24/2023

[6] EUSPA, ENSPACE Enhanced Navigation in Space, Avialble at https://www.euspa.europa.eu/enhanced-navigation-space, Accessed on 05/24/2023

[7] Parker, J.J., Dovis, F., Anderson, B., Ansalone, L., Ashman, B., Bauer, F.H., D'Amore, G., Facchinetti, C., Fantinato, S., Impresario, G. and McKim, S.A., 2022, January. The lunar gnss receiver experiment (lugre). In Proceedings of the 2022 International Technical Meeting of The Institute of Navigation (pp. 420-437)

[8] Delépaut, A., Minetto, A., Dovis, F., Melman, F., Giordano, P. and Ventura-Traveset, J., 2022, January. Enhanced GNSS-based positioning in space exploiting inter-spacecraft cooperation. In Proceedings of the 2022 International Technical Meeting of The Institute of Navigation (pp. 530-544)

[9] Giordano, P., Malman, F., Swinden, R., Zoccarato, P. and Ventura-Traveset, J., 2022, January. The Lunar Pathfinder PNT Experiment and Moonlight Navigation Service: The Future of Lunar Position, Navigation and Timing. In Proceedings of the 2022 International Technical Meeting of The Institute of Navigation (pp. 632-642)

[10] Delépaut, A., Giordano, P., Ventura-Traveset, J., Blonski, D., Schönfeldt, M., Schoonejans, P., Aziz, S. and Walker, R., 2020. Use of GNSS for lunar missions and plans for lunar in-orbit development. Advances in Space Research, 66(12), pp.2739-2756

[11] Marquis, W., 2016, September. The GPS Block IIR antenna panel pattern and its use on-orbit. In Proceedings of the 29th International Technical Meeting of the Satellite Division of The Institute of Navigation (ION GNSS+ 2016) (pp. 2896-2909)

[12] Donaldson, J.E., Parker, J.J., Moreau, M.C., Highsmith, D.E. and Martzen, P.D., 2020. Characterization of on-orbit GPS transmit antenna patterns for space users. NAVIGATION: Journal of the Institute of Navigation, 67(2), pp.411-438.

[13] Kaplan, E.D. and Hegarty, C. eds., 2017. Understanding GPS/GNSS: principles and applications. Artech house